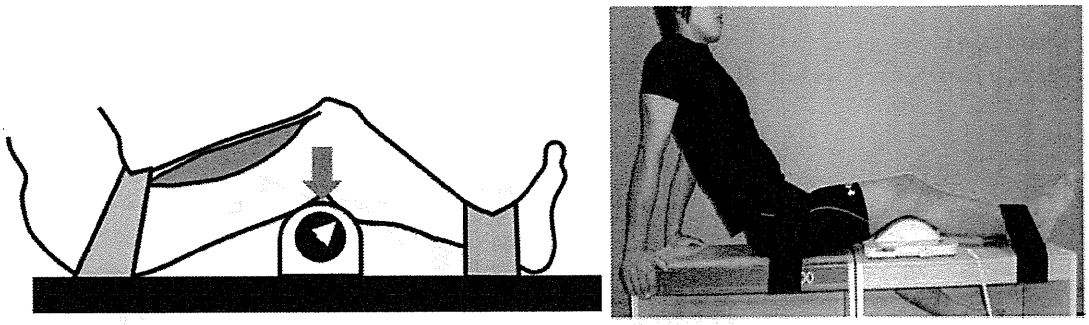

Fig. 2 Position setting of QTM. The subject extends knee on the knee holding part of the QTM. The load pressure applied to the QTM was measured and displayed as the isometric knee extension muscle strength

women, average age: 31.5 ± 8.3 years old). The right knee of all cases was evaluated and measurement was taken regarding 2 sets using both QTM and BIODEX with 5 s of measurement time, taking a break of 20 s in between, and following 5 min of warm-up with an exercise bike at 50w. Moreover, in order to investigate the reproducibility, the order of measurement of QTM and BIODEX was reversed and then the same measurement was conducted again a week following the initial measurement. The maximum measuring value was adopted for both trials, and correlation of the measuring value of QTM and BIODEX was obtained. Regarding the statistical analysis, Pearson's correlation coefficient was used and a level of significance of less than 5 % was determined to have statistical significance.

Relationship between quadriceps strength by QTM and radiographic knee osteoarthritis

The subjects were 1,037 inhabitants (492 men and 535 women) in the Matsudai district in Niigata prefecture and they all participated in an extensive survey of knee OA in 2010 (Matsudai Knee Osteoarthritis Survey). Of 1,037 participants, 21 people were excluded due to data deficiency, and 1,016 subjects (482 men and 534 women) were finally investigated.

Bilateral quadriceps strength of each subject was measured by the QTM. In order to eliminate the effect of physique, measured value was divided by body weight and we evaluated this data as muscle strength per body weight ratio (M/P ratio). Furthermore, a weight-bearing standing knee radiograph was obtained and graded according to the Kellgren–Lawrence classification [23]. Radiographic knee OA was defined if a Kellgren–Lawrence grade of II or higher was detected.

From these results, (1) the change in quadriceps muscle strength level by gender and by age, (2) comparison of the quadriceps muscle strength level between the non-OA group and OA group, and (3) the change in quadriceps muscle strength level by gender and by knee OA grades, were investigated regarding 2,032 knees in 1,016 subjects. Regarding the statistical analysis, a t test without correspondence was used for the investigation by gender and a Student's t test without correspondence as well as analysis of covariance was used for the comparison of the non-OA group and OA group in order to eliminate any effects due to age factors. Moreover, Scheffe's method of paired comparisons was used for the investigation by age and knee OA grade. In all investigations, 5 % or less was determined as the level of significance. All statistical analyses were performed using SPSS version 19.

The study was approved by the Ethics Committee of our University School of Medicine (receipt number 978, 979).

Results

Validity and reliability of QTM

The correlation of maximum measuring value between QTM and BIODEX was $r = 0.69$ ($p < 0.01$) upon the first measurement and $r = 0.82$ ($p < 0.01$) upon the second measurement conducted the following week, with significant correlation observed at both measurements (Fig. 3). Moreover, a good correlation was also observed between the first and second measured QTM value, at $r = 0.92$ ($p < 0.01$).

Relationship between quadriceps strength by QTM and radiographic knee osteoarthritis

In the Matsudai Knee Osteoarthritis Survey, the average age of the 1,016 subjects was 65.9 ± 13.0 years old (men: 66.9 ± 13.1 years old, women: 64.9 ± 12.7 years old) with most males and females in their seventies, followed by subjects in their sixties and fifties.

Moreover, there were more women subjects in all age groups except for the forties and eighties or older, in which there were more men than women. The prevalence of

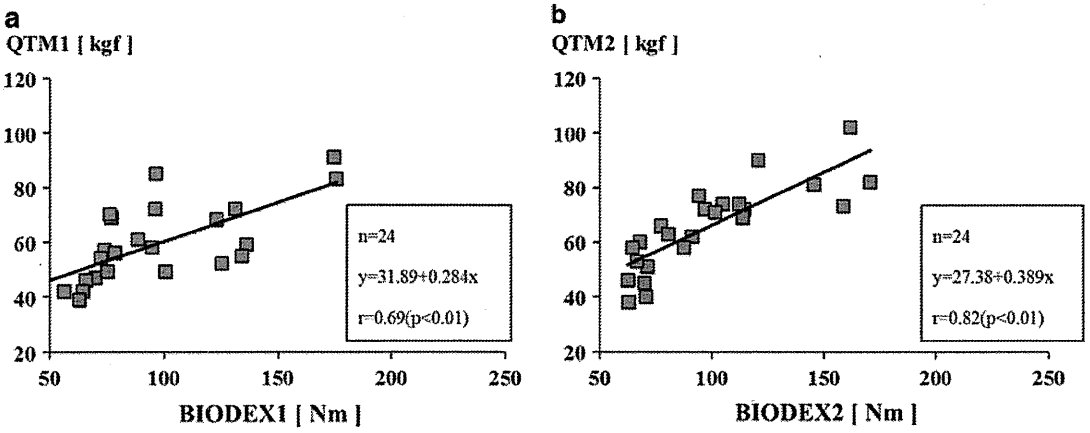

Fig. 3 Correlation of maximum measuring value between QTM and BIODEX. **a** First measurement, **b** second measurement. The correlation between QTM and BIODEX was $r = 0.69$ ($p < 0.01$) upon the first measurement and $r = 0.82$ ($p < 0.01$) upon the second measurement, with significant correlation observed at both measurements

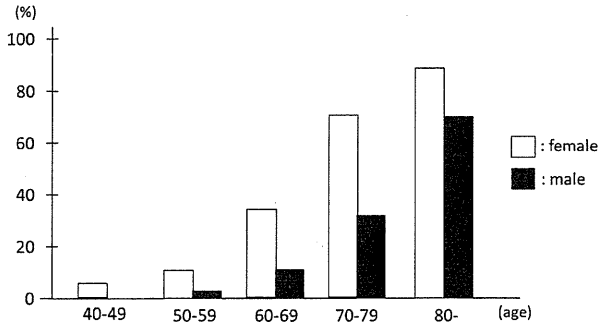

Fig. 4 Prevalence of radiographic knee OA (grade-II or higher upon Kellgren–Lawrence classification) by age

radiographic OA upon Kellgren–Lawrence classification by age when grade II or higher was: 13, 36.9, 67.8, and 86.5 %, regarding women in their fifties, sixties, seventies, and eighties, respectively, and was 1.7, 13.4, 33.5, and 66.2 % in men. The prevalence in women exceeded that of men in all age groups of 40 years old or older (Fig. 4).

Regarding the change in quadriceps muscle strength level by age, differences due to age were not observed in either men or women until the forties; however, the muscle strength level declined with age following 50 years of age, and a significant decline in the muscle strength level was observed in both men and women in their sixties and seventies. Moreover, the level of muscle strength of men in their fifties, sixties, and seventies was significantly higher than that of women (Fig. 5). Knee OA grades 0 and I were classified into the non-OA group and grades II, III, and IV were classified into the OA group by Kellgren–Lawrence classification, and when the muscle strength level was compared between these two groups, a significant decline in the muscle strength level was observed in the OA group in both men and women (Fig. 6). Furthermore, a tendency of the quadriceps muscle strength level to decline with the progression of knee OA grade was observed in both men and women, and particularly, a significant decline was observed between grade 0 and grade I in both men and women and between grade I and grade II in men (Fig. 7).

Fig. 5 Quantitative quadriceps muscle strength by age

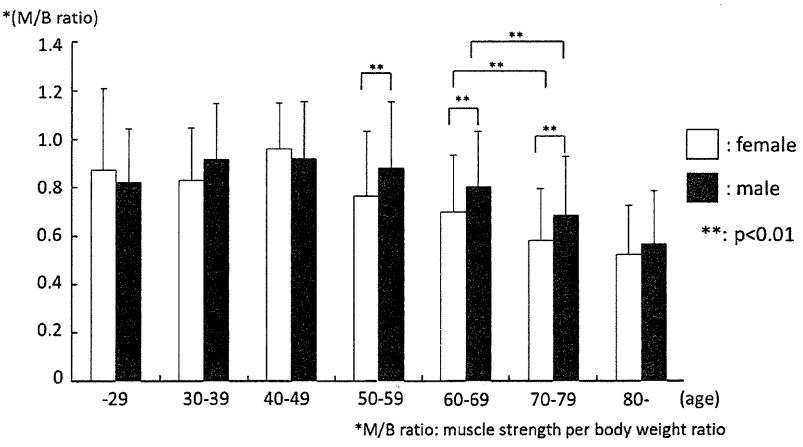

Discussion

In the present study, we showed the clinical utility of the QTM and clarified the relationship between radiographic knee osteoarthritis and quantitatively evaluated quadriceps muscle strength.

Currently, isokinetic devices such as Cybex, Biodex, and KIN-COM (Chattex, Hixson, TN) allow for the most detailed measurement regarding the quantitative evaluation of the muscular strength of the lower limbs; however, these are expensive, large-scale, and impossible to move. Meanwhile, the Hand Held Dynamometer (HDD) is often used as a portable muscle strength dynamometer, but problems such as a limited dynamometry value have been suggested even though credibility is obtained [24, 25]. Moreover, although there are also chair-shaped measuring training devices that apply a leg press, these have problems with portability due to their weight [26]. The QTM of the current study has higher usability compared to other devices in terms of its small size, light weight, and good portability, as well as the fact that it has good correlation with Biodex and high credibility of measurement, and furthermore, the fact that it comprises not only the muscle strength measuring function but also muscle strength training functions and body composition evaluating functions. Accordingly, it is believed that this device may be actively used in investigational research and muscular strength training guidance with groups other than medical institutes such as sites of epidemiological surveys, nursing homes, and schools.

There are several epidemiological studies regarding the relationship between knee OA and quantitatively evaluated quadriceps muscle strength. Slemenda et al. [16] measured the quadriceps muscle strength of 342 people using KIN-COM and reported that the muscle strength to body weight ratio of women with knee OA declined by 15 % compared to that of healthy individuals. Moreover, Baker et al., evaluated quadriceps muscle strength using a chair-shaped measuring device with strain gauge in an epidemiological survey with 2,472 people as the subjects in Beijing, China, and showed that reduced quadriceps muscle strength was correlated to both tibiofemoral and patellofemoral OA in both men and women [27]. Recently, Segal et al., measured quadriceps muscle strength and hamstring muscular strength using Cybex 350 in a multi-institute knee OA study (MOST Study) in the United States and evaluated 3,865 knees in which observation regarding the change of the joint space was possible for the subsequent 30 months. As a result, it was clarified that the decline in quadriceps muscle strength was related to the joint space narrowing in women [28]. Meanwhile, in Japan, Ikeda et al. [29] measured the volume of the quadriceps muscle using CT regarding 738 young and middle-aged women and showed that there was a relationship between quadriceps muscle atrophy and radiographic knee OA. However, in the ROAD study [2], which is currently the largest cohort study in Japan related to knee OA, the relationship between quadriceps muscle strength and knee OA was not mentioned.

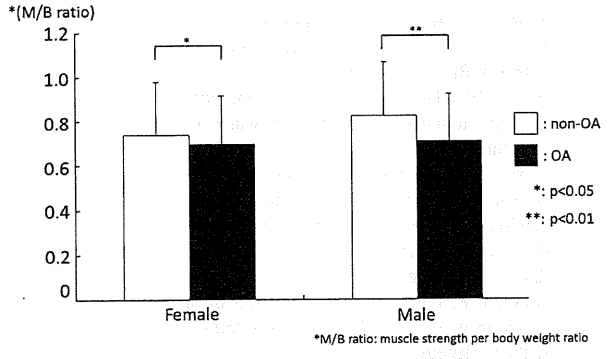

Fig. 6 Comparison of quadriceps muscle strength between non-OA group (K-L grade 0, I) and OA-group (K-L grade II, III, and IV)

Fig. 7 Change of quadriceps muscle strength by knee OA grade

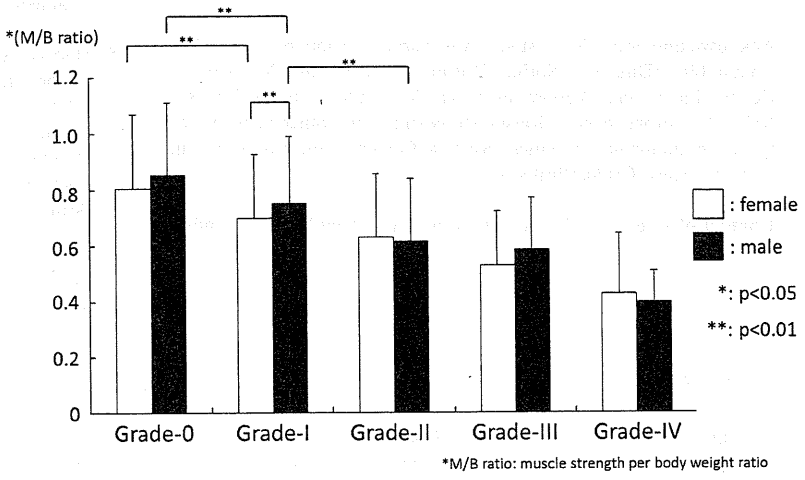

In the current study, the relationship between radiographic knee OA and quantitative quadriceps muscle strength in an epidemiological survey using multiple cases was evaluated. Moreover, the prevalence of radiographic OA in the Matsudai Knee Osteoarthritis Survey was the same as that described in other reports, and from this fact, the results obtained from analysis of the present cohort are, therefore, suggested to be valid as data showing the pathophysiology of knee OA. Quadriceps muscle strength of the OA group was observed to be declining more in both men and woman compared to the non-OA group in this study. This suggests that there is a correlation between knee OA and the decline in quadriceps muscle strength; it was clarified that knee OA in Japan comprised the same pathophysiology as knee OA in other countries regarding quadriceps muscle strength. Furthermore, a significant decline in muscle strength was observed from grade 0 to I and from grade I to II, and it may be said that the fact that a significant change was not observed from grade II to III or from grade III to IV suggests that the decline in quadriceps muscle strength is more strongly related to the incidence of knee OA than to its progression. However, Segal and Glass [30] described in a recent review that reinforcement of quadriceps muscle strength is effective in decreasing the risk of symptomatic knee OA, but there is no evidence regarding whether or not it affects the onset of radiographic knee OA.

There were two limitations in the present study. First, this study was a cross-sectional study and the causal relationship between knee OA and quadriceps muscle strength has not been clarified. Second, the investigation was only conducted regarding radiographic knee OA, not for symptomatic knee OA. It is believed that longitudinally analyzing the same cohorts and investigating whether or not a decrease in quadriceps muscle strength is the cause of incidence or progression of knee OA in addition to conducting the same investigation regarding symptomatic knee OA will be necessary in the future.

Acknowledgments This study was partially supported by H20-Chouju-009 (Director, Noriko Yoshimura) from the Ministry of Health, Labor and Welfare in Japan. The authors thank Takeshi Kaburaki, Hiroko Aouda, Katsutoshi Nishino, and other members of the rehabilitation unit of Niigata Medical Center for their assistance in Matsudai Knee Osteoarthritis Survey.

Conflict of interest The authors declare that they have no conflict of interest.

References

1. Dillon CF, Rasch EK, Gu Q, Hirsch R. Prevalence of knee osteoarthritis in the United States: arthritis data from the third National Health and Nutrition Examination Survey 1991–94. J Rheumatol. 2006;33:2271–9.
2. Yoshimura N, Muraki S, Oka H, Mabuchi A, En-Yo Y, Yoshida M, Saika A, Yoshida H, Suzuki T, Yamamoto S, Ishibashi H, Kawaguchi H, Nakamura K, Akune T. Prevalence of knee osteoarthritis, lumber spondylosis, and osteoporosis in Japanese men and women: the research on osteoarthritis/osteoporosis against disability study. J Bone Miner Metab. 2009;27:620–8.
3. Felson DT, Naimark Anderson J, Kazis L, Castelli W, Meenan RF. The prevalence of knee osteoarthritis in the elderly. Arthritis Rheum. 1987;30:914–8.
4. Anderson JJ, Felson DT. Factors associated with osteoarthritis of the knee in the first National Health and Nutrition Examination Survey (HANES I). Am J Epidemiol. 1988;128:179–89.
5. Zhang Y, Xu L, Nevitt MC, Aliabadi P, Yu W, Qin M, Lui LY, Felson DT. Comparison of the prevalence of knee osteoarthritis between the elderly Chinese population in Beijing and whites in the United States: The Beijing Osteoarthritis Study. Arthritis Rheum. 2001;44:2065–71.
6. Davis MA, Ettinger WH, Neuhaus JM, Hauck WW. Sex difference in osteoarthritis of the knee. The role of obesity. Am J Epidemiol. 1988;127:1019–30.
7. Hart DJ, Doyle DV, Spector TD. Incidence and risk factors for radiographic knee osteoarthritis in middle-aged women. Arthritis Rheum. 1999;42:17–24.
8. Reijman M, Pols HA, Bergink AP, Hazes JM, Belo JN, Lievense AM, Bierma-Zeinstra SM. Body mass index associated with onset and progression of osteoarthritis of the knee but not of the hip: the Rotterdam study. Ann Rheum Dis. 2007;66:158–62.
9. Felson DT, Anderson JJ, Naimark A, Hannan MT, Kannel WB, Meenan RF. Does smoking protect against osteoarthritis? Arthritis Rheum. 1989;32:166–72.
10. Wilder FV, Hall BJ, Barrett JP. Smoking and osteoarthritis: Is there an association? The Clearwater osteoarthritis study. Osteoarthr Cartil. 2003;11:29–35.
11. Felson DT, Hannan MT, Naimark A, Berkeley J, Gordon G, Wilson PWF, Anderson J. Occupational physical demands, knee bending, and knee osteoarthritis: results from the Framingham study. J Rheumatol. 1991;18:1587–92.
12. Zhang Y, Hunter DJ, Nevitt MC, Xu L, Niu J, Lui LY, Yu W, Aliababi P, Felson DT. Association of squatting with increased prevalence of radiographic tibiofemoral knee osteoarthritis. Arthritis Rheum. 2004;50:1187–92.
13. Thelin N, Holmberg S, Thelin A. Knee injuries account for the sports-related increased risk of knee osteoarthritis. Scand J Med Sci Sports. 2006;16:329–33.
14. Segawa H, Omori G, Koga Y. Long-term results of non-operative treatment of anterior cruciate ligament injury. Knee. 2001;8:5–11.
15. Hart DJ, Doyle DV, Spector TD. Association between metabolic factors and knee osteoarthritis in women: the Chingford study. J Rheumatol. 1995;22:1118–22.
16. Slemenda C, Heilman DK, Brandt KD, Katz BP, Mazzuca SA, Braunstein EM, Byrd D. Reduced quadriceps strength relative to body weight. A risk factor for knee osteoarthritis in women? Arthritis Rheum. 1988;11:1951–9.
17. Muzzuca SA, Brandt KD, Dieppe PA, Doherty M, Katz BP, Lane KA. Effect of alignment of the medial tibial plateau and X-ray beam on apparent progression of osteoarthritis in the standing anteroposterior knee radiograph. Arthritis Rheum. 2001;44:1786–94.
18. Sharma L, Song J, Felson DT, Cahue S, Shamiyeh E, Dunlop DD. The role of knee alignment in disease progression and functional decline in knee osteoarthritis. JAMA. 2001;286:188–95.
19. Hochberg MC, Lethbridge-Cejku M, Tobin JD. Bone mineral density and osteoarthritis: data from the Baltimore longitudinal study of aging. Osteoarthr Cartil. 2004;12:45–8.

20. Zhang Y, Hannan MT, Chaisson CE, McAlindon TE, Evans SR, Aliabadi P, Levy D, Felson DT. Bone mineral density and risk of incident and progressive radiographic knee osteoarthritis in women: the Framingham study. J Rheumatol. 2000;27:1032–7.
21. Zhang Y, McAlindon TE, Hannan MT, Chaisson CE, Klein R, Wilson PW, Felson DT. Estrogen replacement therapy and worsening of radiographic knee osteoarthritis. Arthritis Rheum. 1998;41:1867–73.
22. Peach CA, Carr AJ, Loughlin J. Recent advances in the genetic investigation of osteoarthritis. Trends Mol Med. 2005;11:186–91.
23. Kellgren JH, Lawrence JS. Osteo-arthrosis and disk degeneration in the urban population. Ann Rheum Dis. 1958;17:388–97.
24. Kellin BM, Mckeon PO, Gontkof LM, Hertel L. Hand-held dynamometry: reliability of lower extremity muscle testing in healthy, physically active, young adults. J Sport Rehabil. 2008;17:160–70.
25. Knols RH, Aufdemkampe G, Bruin ED, Uebelhart D, Aaronson NK. Hand-held dynamometry in patients with haematological malignancies: measurement error in the clinical assessment of knee extension strength. BMC Musculoskelet Disord. 2009;10:31–41.
26. Palmier-Smith RM, Thomas AC, Gutierrez CK, Sowers MF. Isometric quadriceps strength in women with mild, moderate, and severe knee osteoarthritis. Am J Phys Med Rehabil. 2010;89:541–8.
27. Baker KR, Ling Xu, Zhang Y, Nevitt M, Niu J, Alibadi P, Yu W, Felson DT. Quadriceps weakness and its relationship to tibiofemoral and patellofemoral knee osteoarthritis in Chinese: the Beijing osteoarthritis study. Arthritis Rheum. 2004;50:1815–21.
28. Segal NA, Glass NA, Torner J, Yang M, Felson DT, Sharma L, Nevitt M, Lewis CE. Quadriceps weakness predicts risk for knee joint space narrowing in women in the MOST cohort. Osteoarthr Cartil. 2010;18:769–75.
29. Ikeda S, Tsumura H, Torisu T. Age-related quadriceps-dominant muscle atrophy and incident radiographic knee osteoarthritis. J Ortop Sci. 2005;10:121–6.
30. Segal NA, Glass NA. Is quadriceps muscle weakness a risk factor for incident or progressive knee osteoarthritis? Phys Sportsmed. 2011;39:44–50.

Recurrent knee valgus deformity in Ellis–van Creveld syndrome

Aki Fukuda, Ko Kato, Masahiro Hasegawa, Akinobu Nishimura, Akihiro Sudo and Atsumasa Uchida

We report a case of recurrent knee valgus deformity in a patient with Ellis–van Creveld syndrome. Varus osteotomy, distraction osteogenesis, or epiphyseal stapling is one treatment option for valgus malalignment to improve appearance, gait, and function. However, surgical correction of valgus knee deformity by varus osteotomies of the proximal tibia was not maintained postoperatively, necessitating additional varus osteotomies of the distal femur in this case. The main cause of recurrence was attributed to large bony defect of the anterior segment of the proximal tibia, in addition to depression of the lateral tibial plateau. *J Pediatr Orthop B* **21:352–355 © 2012 Wolters Kluwer Health | Lippincott Williams & Wilkins.**

Journal of Pediatric Orthopaedics B 2012, 21:352–355

Keywords: Ellis–van Creveld syndrome, knee valgus deformity, recurrence

Department of Orthopaedic Surgery, Mie University Graduate School of Medicine, Edobashi, Tsu City, Mie, Japan

Correspondence to Aki Fukuda, MD, Department of Orthopaedic Surgery, Mie University Faculty of Medicine, 2-174 Edobashi, Tsu city, Mie 514-8507, Japan
Tel: +81 59 231 5022; fax: +81 59 231 5211;
e-mail: aki0611@clin.medic.mie-u.ac.jp

Introduction

Ellis–van Creveld syndrome is a rare autosomal recessive disorder characterized by chondrodystrophy, postaxial polydactyly, ectodermal dysplasia, and cardiac anomalies [1]. The syndrome involves numerous anomalies including short-limb dwarfism, postaxial polydactyly, congenital heart defects, hypoplastic nails and teeth, narrow thorax, and valgus knee.

The deformities, particularly valgus knee deformity and dislocation of the patella, often require surgical treatment. Osteotomy, distraction osteogenesis, or epiphyseal stapling is one treatment option for valgus malalignment to improve appearance, gait, and function [2,3]. However, recurrence is frequent because of depression of the lateral tibial plateau in patients with Ellis–van Creveld syndrome [4–6].

Here we report a case of recurrent knee valgus deformity in a patient with Ellis–van Creveld syndrome. The cause of this deformity was attributed to a large bone defect of the anterolateral segment of the proximal tibia.

Case report

An 8-year-old girl (weight, 12 kg; height, 111 cm) presented with severe valgus deformity in both legs. She was diagnosed with Ellis–van Creveld syndrome immediately after the birth. She showed postaxial polydactyly of both hands and congenital heart defects including atrial septal defect. Both hands were operated on at the age of 1 year, and heart surgery was performed at the age of 5 years. Valgus deformity developed in both legs at the age of 2 years. Valgus deformity progressively worsened despite the use of an orthosis. She was examined in our clinic in August 1997 at the age of 7 years because of severe gait disturbance and progressive pain in both knees.

Physical examination of both knees showed full range-of-motion with no effusion. Slight tenderness was present in patellofemoral joint of both knees. Valgus deformity was markedly worsened with knee extension. Both patellae were dislocated laterally. Plain radiographs of both knee joints showed valgus deformity with depression of the lateral aspect of the tibial plateau and hypoplasia of the lateral femoral condyle. Femorotibial angle was 156° in the right knee and 155° in the left (Fig. 1). She underwent bilateral varus dome osteotomies of the proximal tibiae with K-wire at the age of 8 years. Femorotibial angle after surgery improved to 183° in the right knee and 172° in the left (Fig. 2). However, valgus deformity progressively worsened again and femorotibial angle was 154° in the right knee and 150° in the left at the age of 13 years (Fig. 3). Both patellae remained dislocated. Computed tomography of both knee joints showed bilateral dislocation of the patella and large defect of the anterolateral segment of the proximal tibia (Fig. 4). She underwent bilateral varus closed-wedge osteotomies of the distal femora with K-wire and plate and lateral retinacular release combined with medial reefing at the age of 13 years.

At the final follow-up 13 years after first surgery, at the age of 21 years, the patient exhibited significant improvement in the alignment of both legs and function. Clinical evaluation showed more than 120° of flexion and 0° of extension in both knee joints. Walking ability improved markedly, although she reported slight pain in both knee joints. She was able to participate in recreational sports. Plain radiographs of both knee joints showed that femorotibial angle was 177° in the right knee and 176° in

1060-152X © 2012 Wolters Kluwer Health | Lippincott Williams & Wilkins

DOI: 10.1097/BPB.0b013e328345d929

Fig. 1

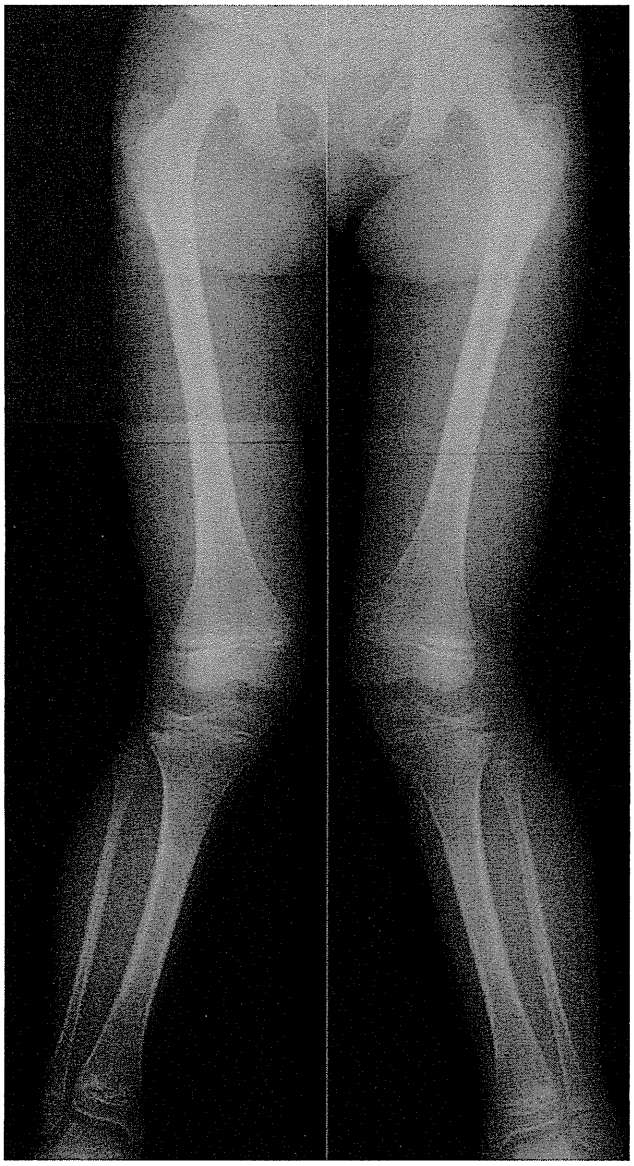

Preoperative plain radiography of both limbs at the age of 8 years.

Fig. 2

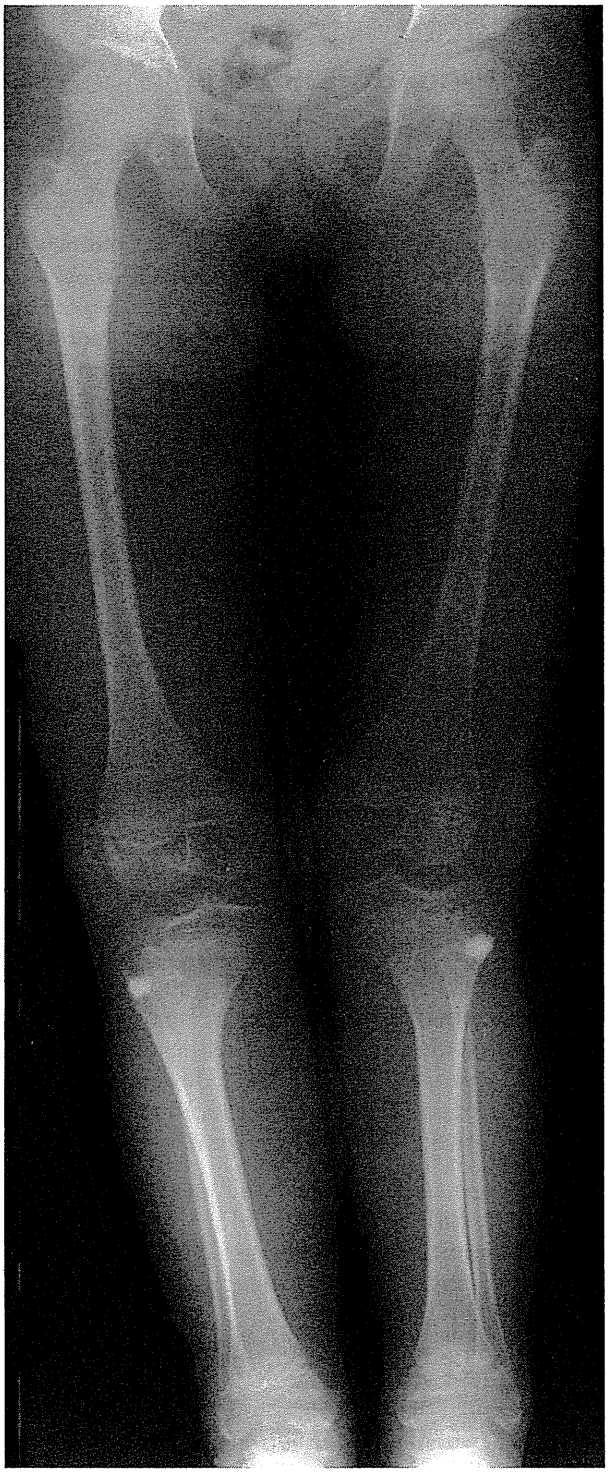

Plain radiography of both limbs after varus osteotomies of the proximal tibiae.

the left (Fig. 5). Bilateral patellae were sufficiently reduced. Alignment of both legs was improved, but depression of the lateral aspect of the tibial plateau and incongruity of both knee joints still existed.

Discussion

Ellis–van Creveld syndrome, also called chondroectodermal dysplasia or mesoectodermal dysplasia, is a rare genetic disorder resulting in skeletal dysplasia. This syndrome was described by Ellis and van Creveld in 1940 and comprises a tetrad of clinical manifestations such as chondrodystrophy, postaxial polydactyly, ectodermal dysplasia, and cardiac defects. Associated abnormalities were found in this case, such as short stature, short limbs, postaxial polydactyly, hypoplastic nails and teeth, narrow thorax, valgus knee deformity, and congenital heart defects such as atrial septal defect.

Fig. 3

Plain radiography of both limbs at the age of 13 years.

Fig. 4

Three-dimensional computed tomography showed bilateral dislocation of the patellae and a large defect of the anterolateral segment of the proximal tibia.

The distal limbs are more affected than the proximal limbs in Ellis–van Creveld syndrome. Radiographically, all tubular bones in the extremities are short and thick [7]. The proximal tibial epiphyses are particularly small, medially displaced, and flattened. Hypoplasia of the lateral tibial plateau with depression was responsible for the valgus knee deformity.

From an orthopedic perspective, severe valgus knee deformity and patellar dislocation require surgical treatment to

Fig. 5

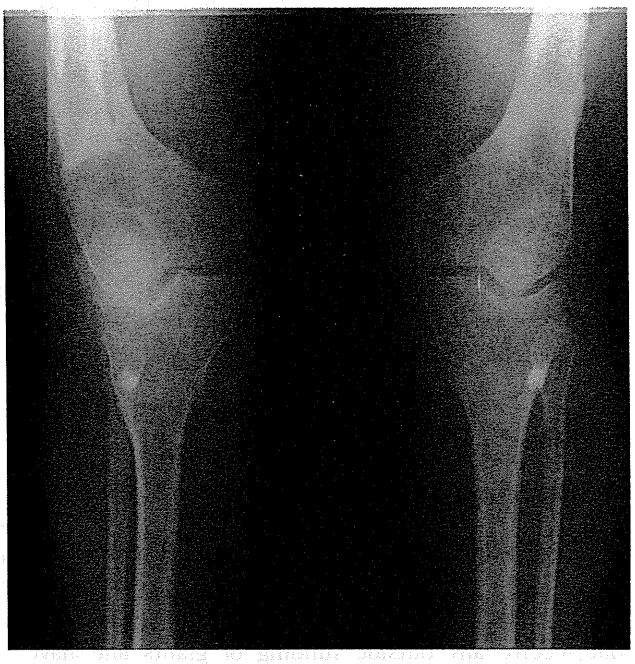

Plain radiographs of both limbs at the age of 21 years.

improve appearance, gait, and function. Osteotomy, distraction osteogenesis, or epiphyseal stapling are treatment options to improve the femorotibial axis. However, complications such as recurrence, nonunion, fracture, and peroneal nerve palsy are reported after correction of valgus knee deformity in patients with Ellis–van Creveld syndrome [4–6]. Neurovascular complications have been reported as high as 20% after osteotomy of the tibia in children [3]. Shibata *et al.* [4] reported a recurrent case and a case with transient peroneal nerve palsy after lateral soft tissue release and corrective osteotomy of the tibia. Undercorrection is reportedly frequent because of joint surface incongruity and depression of the lateral tibial plateau. Conversely, Morsy *et al.* [8] reported excellent results of one-stage femoral and tibial correction of valgus knee deformities with an Ilizarov external fixator. Valgus knees were reportedly sufficiently corrected with no nerve palsy, no recurrence, and no refracture at the osteotomy site. In this case, surgical correction of valgus knee deformity by varus osteotomies of the proximal tibia was not maintained postoperatively, necessitating additional varus osteotomies of the distal femur. The main cause of valgus deformity in Ellis–van Creveld syndrome is depression of the lateral aspect of the tibial plateau and soft tissue tightness including the fascia lata, lateral collateral ligament, biceps femoris, gastrocnemius, and capsule. In this case, recurrent knee valgus deformity was secondary to hypoplasia of the lateral tibial and femoral condyle. In addition, valgus instability may be attributed to large bony defect of the anterior segment of the proximal tibia in full extension of the knee and loosening

of the medial collateral ligament after overcorrection by varus osteotomies of the proximal tibia. These findings suggest that one-stage osteotomy at both femoral and tibial sites, as reported by Morsy, should be considered to prevent recurrence in the case of severe valgus knee deformity combined with patellar dislocation in patients with Ellis–van Creveld syndrome.

We have reported a case of severe valgus knee deformity and patellar dislocation in patients with Ellis–van Creveld syndrome. This recurrent knee valgus deformity was attributed to large bony defect of the anterior segment of the proximal tibia, in addition to depression of the lateral tibial plateau.

Acknowledgements

The authors certify that his or her institution has approved the human protocol for this study and that all studies were conducted in conformity with ethical principles of research, and that informed consent was obtained. The authors did not receive any outside funding or grants and have no commercial associations that might pose a conflict of interest in connection with submitted article.

Conflicts of interest

There are no conflicts of interest.

References

1 Ellis RWB, van Creveld S. A syndrome characterized by ectodermal dysplasia, polydactyly, chondrodysplasia and congenital morbus cordis. Report of three cases. *Arch Dis Child* 1940; **15**:65.
2 Zuege RC, Kempken TG, Blount WP. Epiphyseal stapling for angular deformity at the knee. *J Bone Joint Surg Am* 1979; **61**:320–329.
3 Steel HH, Sandrow RE, Sullivan PD. Complications of tibial osteotomy in children for genu varum or valgum. Evidence that neurological changes are due to ischemia. *J Bone Joint Surg Am* 1971; **53**:1629–1635.
4 Shibata T, Kawabata H, Yasui N, Nakahara H, Hirabayashi S, Nakase T, Ochi T. Correction of knee deformity in patients with Ellis–van Creveld syndrome. *J Pediatr Orthop B* 1999; **8**:282–284.
5 Milgram JW, Bailey JA II. Orthopaeidc aspects of the Ellis–van Creveld Syndrome. *Bull Hosp Jt Dis* 1975; **36**:11–19.
6 Pinelli G, Cottafava F, Senes FM, Becchetti S, Cosso D, Costa M, *et al.* Ellis–van Creveld syndrome: description of four cases. Orthopaedic aspects. *Ital J Orthop Traumatol* 1990; **16**:113–121.
7 Caffey J. Chondroectodermal dysplasia. *Am J Roentgenol* 1952; **68**:875.
8 Morsy A, Tsuchiya H, Matsubara H, Kabata T, Tomita K. Ilizarov deformity correction of the lower limbs in Ellis–van Creveld syndrome. *J Orthop Sci* 2007; **12**:505–509.

Rheumatol Int (2012) 32:1411–1413
DOI 10.1007/s00296-011-1897-8

SHORT COMMUNICATION

A tumor endoprosthesis is useful in elderly rheumatoid arthritis patient with acute intercondylar fracture of the distal femur

Hiroki Wakabayashi · Yohei Naito · Masahiro Hasegawa · Tomoki Nakamura · Akihiro Sudo

Received: 8 November 2010 / Accepted: 13 March 2011 / Published online: 26 March 2011

Abstract The purpose of this paper is to report the use of total knee arthroplasty using a tumor prosthesis in the treatment of elderly patients with an intercondylar fracture of the distal femur. Supracondylar fractures of the femur in patients with rheumatoid arthritis are difficult to treat due to joint deformity. We present outcomes for treating intercondylar fractures of the distal femur in rheumatoid arthritis patient using a tumor endoprosthesis. This technique allows early mobilization of the patient, with restoration of a good range of knee motion. A tumor prosthesis appears to be a viable treatment option for intercondylar femoral fractures in elderly patients. It is well tolerated and permits early ambulation and return to activities of daily living.

Keywords Tumor endoprosthesis · Rheumatoid arthritis · Supracondylar fracture · Distal femur

Introduction

The treatment of fractures around rheumatoid arthritis (RA) joints is difficult because of coexisting RA disease, severe osteopenia, and significant arthritic change. We present outcomes for the treatment of intercondylar fractures of the distal femur in RA patient that allows restoration of a good range of knee motion. It is useful for RA patient with intercondylar fractures, especially in low-demand elderly patient. This report is the second case report that treated acute supracondylar fracture using a tumor endoprosthesis.

H. Wakabayashi (✉) · Y. Naito · M. Hasegawa · T. Nakamura · A. Sudo
Department of Orthopaedic Surgery, Mie University Graduate School of Medicine, 2-174 Edobashi, Tsu, Mie 514-8507, Japan
e-mail: whiroki@clin.medic.mie-u.ac.jp

Case report

A 77-year-old woman was referred to our institute (Institute of Orthopeadic Research) due to progressive pain in both knees and wrists. She was able to walk with a cane. At the age of 70 years, she had been diagnosed with RA and was managed with oral corticosteroid (prednisolone, 5 mg once daily) and an anti-inflammatory drug (meloxicam, 10 mg once daily). She had been treated with DMARD therapy (tacrolimus, 1.5 mg once daily) and had controlled active inflammation. The results of the laboratory investigations were as follows: erythrocyte sedimentation rate, 44 mm; C-reactive protein, 0.36 mg/dl; and matrix metalloprotease, 299 ng/ml.

According to the Steinbrocker classification, she had Stage III and Class III RA. The X-rays of both knees showed narrowing of the joint space and were classified as Larsen grade III. The patient refused total knee arthroplasty (TKA).

She fell at home, sustaining a supracondylar fracture of the left femur. X-ray of the left knee showed intra-articular fractures in 4 parts, classified as Orthopaedic Trauma Association type 33 C2 [1] (Fig. 1a, b).

Surgery was performed in February 2008. The fracture site was identified, and the distal fracture parts were removed via a medial parapatellar approach incision. The length of the femur to be removed was measured using calipers and matched with the available implants. A standard proximal tibial cut was made perpendicular to the mechanical axis using an extramedullary alignment guide. The tibia was prepared using a series of broaches to allow

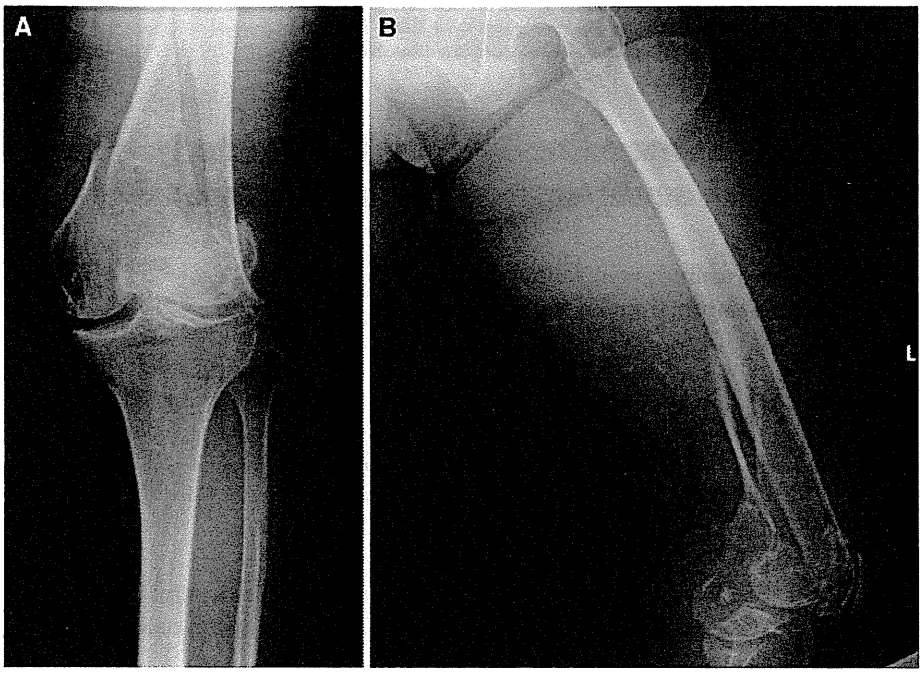

Fig. 1 **a** Anteroposterior and **b** lateral radiographs of the *left* knee before surgery

for acceptance of the stem and the fin. Appropriately sized trial prostheses were implanted, and the limb lengths and patellar tracking were checked. The knee joint and the segmental bone defect were reconstructed using the Kyocera limb salvage (KLS) tumor endoprosthesis.

The left knee was maintained in a no cast brace and mobilized starting 1 day after surgery. Follow-up at 24 months revealed an excellent, pain-free level of function. The left knee had a range of motion of 0–135°, and the patient was able to walk with a cane. The American Knee Society Scores were recorded as 95/100 for the knee score and 65/100 for the functional score. Radiographs demonstrated no evidence of prosthesis loosening or migration and no erosion of the femur or tibia (Fig. 2a, b).

Discussion

Most fractures at the distal end of the femur occur following a blow to the flexed knee in elderly individuals who fall directly onto the knee. The aim of treatment of supracondylar/condylar femoral fractures is to restore function to pre-injury levels. In such cases, the fracture usually involves the joint and is frequently comminuted, often with some bone loss, thus making open reduction and internal fixation difficult.

Rigid fixation is best for early mobilization of the knee. However, in elderly osteopenia patients, rigid fixation often cannot be achieved, and some form of external splinting is also required. Even if rigid fixation can be achieved and early mobilization can be started, full weight bearing should not be allowed for a number of weeks. In cases, where rheumatic osteopenia is so severe that acceptable fixation cannot be achieved and the surface of the joint is so shattered that reconstruction seems foolhardy, it is impossible to secure the fracture adequately to allow knee movement, so adhesions are likely to develop, causing further knee stiffness.

For these fractures, there is a 2-stage procedure. The first surgery requires open reduction and internal fixation. After removal of the fixation devices, a total knee arthroplasty (TKA) can be performed. However, the 2-stage procedure has disadvantages. These patients are at increased risk of restricted motion and perioperative complications following TKA such as skin necrosis and infection. And fracture fixation at the first surgery may make the subsequent TKA difficult because of arthrofibrosis, patella infra, and reduced range of motion [2, 3]. Two-stage procedures would confine patients to bed for a longer time and prolong the duration of treatment. Thus, a primary knee replacement can be used to overcome a problem that is otherwise insurmountable for elderly patients [4–8].

If the fracture site is more proximal and the patient has a reasonable chance of regaining good knee function, the fracture needs to be fixed and the knee replaced. In such cases, a primary knee replacement with a tumor endoprosthesis may be appropriate. In previous reports, a tumor endoprosthesis was used for periprosthetic supracondylar TKA fractures [9, 10], complex TKA revision [11], and failed internal fixation or nonunion of a distal femur

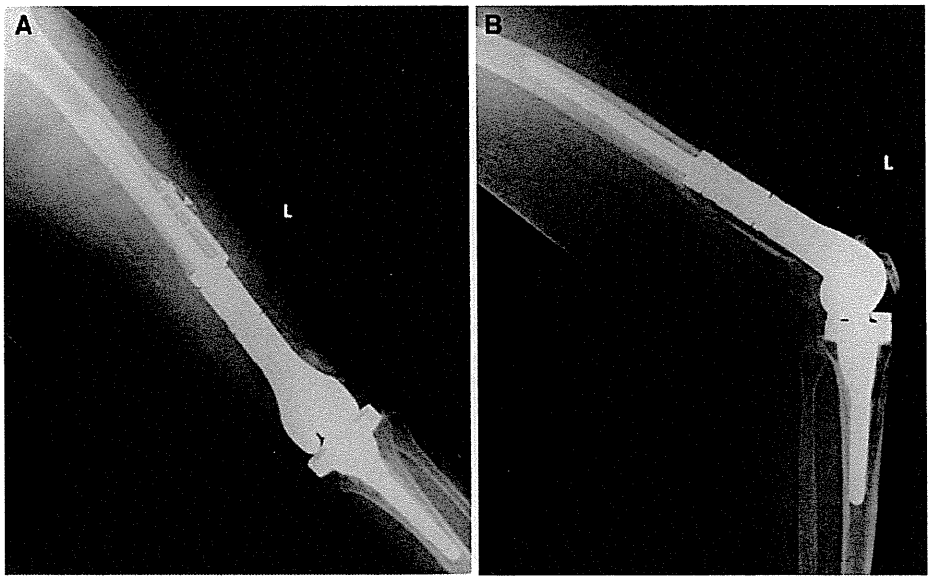

Fig. 2 **a** Anteroposterior and **b** lateral radiographs of the *left* knee 24 months after surgery

fracture [10, 12–14]. There has been only one patient with an acute supracondylar fracture, reported by Freedman et al. [12], which was reconstructed using a tumor endoprosthesis.

We performed replacement using a tumor endoprosthesis because of type C supracondylar fractures with coexisting RA disease, severe osteopenia, and significant arthritic change within the knee joint.

One year after surgery, the present patient underwent TKA surgery for her right knee because she was satisfied with the treatment for the left knee. Despite the operative challenges for an acute fracture, a tumor endoprosthesis provided significant pain relief and functional improvement for an intercondylar fracture of the distal femur.

In RA patient with a fracture at the end of the distal femur, replacement with a tumor endoprosthesis is a new surgical option. We recommend this method in type C supracondylar fractures in which there is coexisting disease or significant arthritic change within the joint.

Conflict of interest The authors have declared no conflict of interest.

References

1. Dislocation Fracture Classification Compendium (2007) Orthopedic trauma association classification, database and outcome comittee. J Orthop Trauma 21(Suppl 10):S1–S163
2. Moore TJ, Watson T, Green SA et al (1987) Complications of surgically treated supracondylar fractures of the femur. J Trauma 27:402–406
3. Yang RS, Liu HC, Liu TK (1990) Supracondylar fractures of the femur. J Trauma 30:315–319
4. Wolfgang GL (1982) Primary total knee arthroplasty for intercondylar fracture of the femur in a rheumatoid arthritic patient. A case report. Clin Orthop Relat Res 171:80–82
5. Newman JH (1990) Supracondylar fractures of the femur. Injury 21:280–282 Review
6. Bell KM, Johnstone AJ, Court-Brown CM et al (1992) Primary knee arthroplasty for distal femoral fractures in elderly patients. J Bone Joint Surg Br 74:400–402
7. Yoshino N, Takai S, Watanabe Y et al (2001) Primary total knee arthroplasty for supracondylar/condylar femoral fracture in osteoarthritic knees. J Arthroplast 16:471–475
8. In Y, Koh HS, Kim SJ (2006) Cruciate-retaining stemmed total knee arthroplasty for supracondylar-intercondylar femoral fractures in elderly patients: a report of 3 cases. J Arthroplast 21:1074–1079
9. Oxborrow NJ, Stone MH (1997) A new method of treatment for periprosthetic supracondylar fractures of the femur for prostheses with a stemmed femoral component. J Arthroplast 12:596–597
10. Springer BD, Sim FH, Hanssen AD et al (2004) The modular segmental kinematic rotating hinge for nonneoplastic limb salvage. Clin Orthop Relat Res 421:181–187
11. Harrison RJ Jr, Thacker MM, Pitcher JD et al (2006) Distal femur replacement is useful in complex total knee arthroplasty revisions. Clin Orthop Relat Res 446:113–120
12. Freedman EL, Hak DJ, Johnson EE et al (1995) Total knee replacement including a modular distal femoral component in elderly patients with acute fracture or nonunion. J Orthop Trauma 9:231–237
13. Davila J, Malkani A, Paiso JM (2001) Supracondylar distal femoral nonunions treated with a megaprosthesis in elderly patients: a report of 2 cases. J Orthop Trauma 15:574–578
14. Haidukewych GJ, Springer BD, Jacofsky DJ et al (2005) Total knee arthroplasty for salvage of failed internal fixation or nonunion of the distal femur. J Arthroplast 20:344–349

Obata et al. Arthritis Research & Therapy 2012, 14:R241
http://arthritis-research.com/content/14/6/R241

arthritis research&therapy

RESEARCH ARTICLE Open Access

Effect of autologous platelet-rich plasma-releasate on intervertebral disc degeneration in the rabbit anular puncture model: a preclinical study

Shuji Obata[1†], Koji Akeda[1*†], Takao Imanishi[1], Koichi Masuda[2], Won Bae[3], Ryo Morimoto[1], Yumiko Asanuma[1], Yuichi Kasai[4], Atsumasa Uchida[1] and Akihiro Sudo[1]

Abstract

Introduction: Platelet-rich plasma (PRP) is a fraction of plasma in which several growth factors are concentrated at high levels. The active soluble releasate isolated following platelet activation of PRP (PRP-releasate) has been demonstrated to stimulate the metabolism of IVD cells in vitro. The in vivo effect of PRP-releasate on degenerated IVD remains unknown. The purpose of this study was to determine the reparative effects of autologous PRP-releasate on degenerated intervertebral discs (IVDs).

Methods: To induce disc degeneration, New Zealand white rabbits (n = 12) received anular puncture in two noncontiguous discs. Autologous PRP and PPP (platelet-poor plasma) were isolated from fresh blood using two centrifugation techniques. Four weeks after the initial puncture, releasate isolated from clotted PPP or PRP (PPP- or PRP-releasate), or phosphate-buffered saline (PBS; control) was injected into the punctured discs. Disc height, magnetic resonance imaging (MRI) T2-mapping and histology were assessed.

Results: Anular puncture produced a consistent disc narrowing within four weeks. PRP-releasate induced a statistically significant restoration of disc height (PRP vs. PPP and PBS, $P<0.05$). In T2-quantification, the mean T2-values of the nucleus pulposus (NP) and anulus fibrosus (AF) of the discs were not significantly different among the three treatment groups. Histologically, the number of chondrocyte-like cells was significantly higher in the discs injected with PRP-releasate compared to that with PBS.

Conclusions: The administration of active PRP-releasate induced a reparative effect on rabbit degenerated IVDs. The results of this study suggest that the use of autologous PRP-releasate is safe and can lead to a clinical application for IVD degeneration.

Introduction

Intervertebral disc (IVD) degeneration is considered to be a multifactorial process involving mechanical, genetic, systemic, and biological factors. Biochemically, IVD degeneration is characterized by a change in extracellular matrix molecules (loss of proteoglycan and water content in the nucleus pulposus, or NP), resulting in an alteration of the biomechanical properties of IVD tissues. These degenerative changes are considered to induce the disruption (radial and circumferential tears, cracking, and fissuring) of IVD tissues, leading to degenerative disc diseases and, eventually, to low back pain [1-4]. Unfortunately, because of the absence of blood supply in the inner anulus fibrosus (AF) and NP, IVD tissues have little potential for self-repair. Thus, experimental treatment options for disc degeneration, encompassing molecular, gene, and cell therapies, are being actively pursued [5].

To develop biological therapies for IVD repair, molecular biology and tissue engineering technologies have recently been applied to improve the micro-environment of IVD tissues [6-14]. Growth factors are biologically active molecules capable of stimulating cellular growth, proliferation, and differentiation in an endocrine or

* Correspondence: k_akeda@clin.medic.mie-u.ac.jp
† Contributed equally
[1]Department of Orthopaedic Surgery, Mie University Graduate School of Medicine, 2-174 Edobashi, Tsu, 514-8507, Japan
Full list of author information is available at the end of the article

paracrine fashion. Many growth factors, such as transforming growth factor-β (TGF-β), insulin-like growth factor-1 (IGF-1), basic fibroblast growth factor, platelet-derived growth factor (PDGF), epidermal growth factor (EGF), and bone morphogenetic protein (BMP)-2 and BMP-7 (otherwise known as osteogenic protein-1, or OP-1), have been shown to positively modulate the extracellular matrix of IVD cells (see review in [15]). Interestingly, in both *in vitro* and animal studies, autologous platelet-rich plasma (PRP), which contains concentrated levels of growth factors and other cytokines, has been shown to provide a 'local environment for tissue regeneration' [16]. Furthermore, the effective role of PRP on tissue repair or regeneration (or both) in a range of tissue types, including bone, cartilage, tendon, and muscle, has been reported (see review in [16]).

The principal function of platelets is to prevent bleeding. Platelets circulating in the blood rapidly adhere to damaged endothelial tissues in response to vessel injury. The activated platelets release plasma coagulation factors and adhesive protein, generating a fibrin clot. In addition, activated platelets release a range of growth factors (for example, IGF-1, TGF-β, PDGF, and EGF), cytokines (for example, interleukin-1β [IL-1β] and IL-8), and angiogenic factors (for example, vascular endothelial growth factor and angiopoietin-1) [17,18]. These biologically active molecules synergically promote hemostasis and tissue repair [17,19]. PRP is a plasma fraction that contains platelets concentrated at a high level. Because activated platelets have the potential to release growth factors, including IGF-1, TGF-β, PDGF, and EGF, PRP has been clinically used to accelerate wound healing and tissue regeneration in orthopedic, oral-maxillofacial, and plastic surgery [17,19,20]. Recently, the active soluble releasate isolated from PRP has been demonstrated to effectively stimulate the metabolism of articular chondrocytes [21] and IVD cells [22]*in vitro*. Therefore, we hypothesized that the administration of PRP-releasate into the degenerated IVD tissue could dramatically change the metabolic homeostasis and micro-environment within the IVD and finally improve the potential for self-repair. The purpose of this study was to determine the reparative effects of the *in vivo* administration of autologous PRP-releasate into degenerated IVDs in a well-established rabbit anular puncture model [23] using radiologic, magnetic resonance imaging (MRI) T2 mapping, and histological analyses.

Materials and methods

Animal surgery and blood sampling

A rabbit anular puncture model of disc degeneration was established, as previously reported [23]. Twelve female New Zealand white rabbits (Kitayama Labes Laboratory Animals Bleeding & Equipment Supply, Ina, Japan), ranging from 2.9 to 3.4 kg in body weight, were used in this study with the approval of our university's Institutional Animal Care and Use Committee. Preoperatively, rabbits were anesthetized by an intramuscular injection of ketamine hydrochloride (25 mg/kg; Ketalar; Sankyo Seiyaku, Tokyo, Japan) mixed with xylazine (5 mg/kg; Celactal; Bayer, Tokyo, Japan). Lateral plain radiographs were obtained to determine baseline IVD height values before puncture. Under general anesthesia with 3.0% isoflurane (Mylan Pharmaceutical Inc., Tampa, FL, USA), lumbar IVDs were exposed through a posterolateral approach, the initial puncture with an 18-gauge needle was performed on two non-contiguous discs (L2/3 and L4/5), and the disc (L3/4) between punctured discs was left intact as a control [11]. During surgery, 10 mL of fresh blood was drawn from the femoral artery with a 21-gauge needle into a syringe treated with 1 mL of anti-coagulant (citrate dextrose-A solution; Terumo, Tokyo, Japan). An additional 5 mL of fresh blood was drawn to isolate autologous serum to use in the activation step. The rabbits were returned to their cages after a short recovery observation and mobilized *ad libitum*.

Preparation of platelet-rich plasma and platelet-poor plasma releasates

PRP and PPP were prepared by using two centrifugation techniques (Figure 1). Whole blood collected by using an anti-coagulant was first centrifuged by using a centrifugation apparatus (Himac CT 6D; Hitachi Ltd., Tokyo, Japan) for 15 minutes at 330*g* to separate plasma and hemocyte fractions. The plasma fraction was then centrifuged for an additional 10 minutes at 1,000*g*. The supernatant plasma (PPP) was carefully removed, and the remaining PPP (approximately 200 μL) and precipitated platelets were designated as PRP. The number of platelets of each whole blood and PRP fraction was counted by using a hemocytometer. Autologous serum was prepared from the coagulated whole blood, which was centrifuged for 10 minutes at 1,000*g*. To activate platelets, PRP and PPP were treated with a mixture of autologous serum and 2% $CaCl_2$ (Otsuka Pharmaceutical, Tokyo, Japan) for clot formation. The clotted PPP and PRP were allowed to rest at room temperature for more than 30 minutes, followed by centrifugation at 1,000*g* for 10 minutes. The resulting soluble releasate from the clot preparation of PRP (PRP-releasate) and PPP (PPP-releasate) was isolated and kept at -80°C until used.

Experimental groups

Four weeks after the initial puncture, phosphate-buffered saline (PBS) (control) or PPP- or PRP-releasate was injected into the punctured discs through a contralateral side approach. The anterolateral surfaces of the previously punctured discs (L2/3-L4/5) were exposed

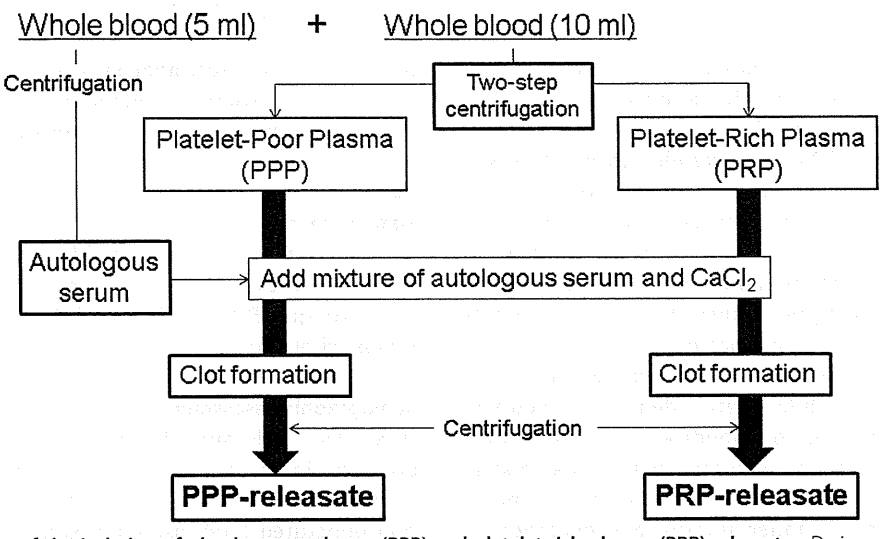

Figure 1 Flowchart of the isolation of platelet-poor plasma (PPP) and platelet-rich plasma (PRP) releasates. During surgery, a total of 15 mL of whole blood was drawn from the femoral artery. PPP and PRP were prepared by using two separate centrifugation techniques. Five milliliters of whole blood was used for isolating autologous serum. After clot formation by adding autologous serum and $CaCl_2$, the PPP- and PRP-releasates were isolated from the clotted PPP and PRP by centrifugation.

with confirmation of osteophyte formation. Twelve rabbits were divided into two groups. One group (n = 4) received an injection of PBS (20 μL) at L2/3 and L4/5 discs into the center of the NP by using a 30-gauge needle. For the remaining rabbits (n = 8), each rabbit received one injection of PRP (20 μL) and one injection of PPP (20 μL) randomly given between L2/3 and L4/5. All preoperative and postoperative care was performed as in the initial operation.

Radiographic analysis of disc height

Lateral plain radiographs of the lumbar spine were taken after administration of ketamine hydrochloride (25 mg/kg) and xylazine (5 mg/kg) at 2-week intervals up to 12 weeks after the initial puncture. Extreme care was taken to maintain a consistent level of anesthesia during radiography of each animal and at each time to obtain a similar degree of muscle relaxation, which may affect the disc height. All radiographic images were independently analyzed by using OsiriX Medical Image software (OsiriX Foundation, Geneva, Switzerland) by an orthopedic researcher who was blinded to the treatment groups. Data are reported as the IVD height expressed as the disc height index (DHI) (DHI = IVD height/adjacent vertebral disc height) [11,23]. Change in the DHI of injected discs was expressed as percentage DHI (% DHI) and normalized to the measured preoperative IVD height: % DHI = (postoperative DHI/preoperative DHI) × 100 [11]. Non-responsive treated discs (which did not exhibit degenerated changes at 4 weeks) were excluded from the analysis.

Magnetic resonance imaging T2 quantification

Twelve weeks after the initial puncture, all rabbits were sacrificed and the spinal columns (L1 to L6 vertebra) with surrounding soft tissues were isolated and subjected to quantitative T2 MRI analysis. MRI was performed by using a 3.0-Tesla imager (Achieva 3.0T; Philips, Amsterdam, The Netherlands) with a 3-inch birdcage extremity coil (Philips). Quantitative T2 mapping was performed by using a multi-echo spin-echo sequence in the sagittal plane. Scanning parameters were the following: time-to-repeat (TR) = 3,000 ms, time-to-echo (TE) = 20, 40, 400 ms (20 TEs), field of view = 10 cm, slice thickness = 2 mm, image matrix = 560 × 560, and number of excitation = 1. Total scanning time per sample was 10 minutes 39 seconds. For creating color-coded T2 maps, MRI images at multiple TE were imported into OsiriX Medical Image software with T2 mapping plug-in.

The regions of interest (ROIs) for the NP were defined on T2-weighted images taken at a TE of 100 ms, whereas the ROIs for the AF were defined on proton density-weighted images taken at a TE of 20 ms. These images were selected to best visualize the borders of the AF and NP. Signal intensity values within each ROI were averaged and then fit mono-exponentially to a T2 decay equation. To minimize the differences between animals, the T2 values of each experimental disc were normalized by that of the non-punctured disc (L3/4). Non-responsive treated discs (which did not exhibit degenerated MR morphology) were excluded from the analysis (PBS group; n = 7 discs, PPP group; n = 7 discs, PRP group; n = 8 discs).

Histological examination

After MRI assessment, the experimental IVDs were excised from the vertebral body-disc-vertebral body unit, and each IVD was fixed in 4% paraformaldehyde for 7 days at 4°C and then decalcified in 0.5 M ethylenediaminetetraacetic acid (EDTA), embedded in paraffin, sectioned, and assessed by conventional histology. Midsagittal sections (5 μm) of each IVD were stained with either hematoxylin and eosin or with safranin-O. Blinded to the experiment, an observer analyzed the histological sections and graded them by using the recently established histology grading protocol [24].

The chondrocyte-like cells appeared as large cells encircled with pericellular matrix densely stained with safranin-O. The number of chondrocyte-like cells (more than 2.0 μm in diameter including pericellular matrix) in the serial sections (100 μm in width from upper to lower endplate) of the inner anterior and posterior AF, and the center of the NP was quantified by manually counting the cells by using a light microscope.

Statistical analysis

The significance of differences among means of data on radiograph measurements was analyzed by two-way repeated measures analysis of variance (ANOVA). T2 values in MRI and the number of chondrocyte-like cells were analyzed by one-way ANOVA and Fisher's protected least significant difference as a *post hoc* test. The data are expressed as the mean ± standard error of the mean. Histology grading was analyzed by the Kruskal-Wallis test and Mann-Whitney *U* test for the effect of treatment. Statistical analysis was performed by using the StatView program (version 5.0; SPSS Inc., Chicago, IL) with a significance level of P of less than 0.05.

Results

Platelet count

The mean platelet count of PRP was about 29 times greater than that of whole blood (whole blood: 195.2 ± 6.4 × 10^3/μL, PRP: 5,752.5 ± 393.7 × 10^3/μL, P <0.01 versus whole blood).

Radiographic assessment

In all PBS, PPP, and PRP groups, radiographs 4 weeks after the initial anular puncture showed a significant narrowing of disc height compared with that of the non-punctured L3/4 disc (approximately 24.0% decrease compared with the baseline percentage DHI values before anular puncture, P <0.01) (Figure 2, see arrow). There were no significant differences in the percentage DHI among the experimental groups.

The treatment significantly affected the post-injection disc height (two-way repeated ANOVA, P <0.001). Two weeks after the injection of PPP- or PRP-releasate, the disc height began to recover compared with the discs injected with PBS (% DHI: PBS group: 70.8% ± 1.5%; PPP group: 83.7% ± 3.0%, P <0.01; PRP group: 86.8% ± 9.3%, P <0.01 all versus PBS group) (Figure 2). Four

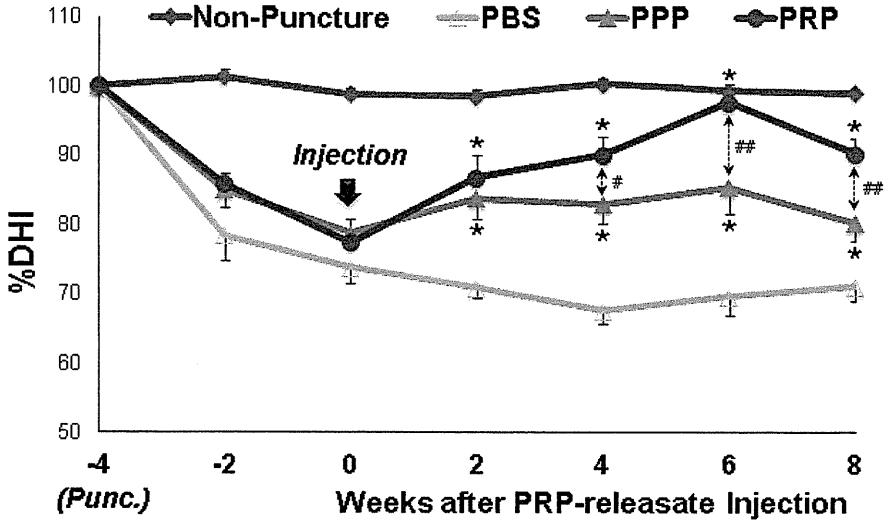

Figure 2 Changes in the intervertebral disc height index (DHI). Four weeks after anular puncture [Punc. (at -4 weeks)], phosphate-buffered saline (PBS) (control) or platelet-poor plasma (PPP)- or platelet-rich plasma (PRP)-releasate was injected into the punctured discs. The percentage DHI was measured at each time point to quantify changes in disc height. Four weeks after the injection of PRP-releasate, the percentage DHI of injected discs in the PRP group was significantly higher than that in the PBS group (P <0.01, repeated analysis of variance). This significant difference in the percentage DHI was sustained until 8 weeks after the injection. Values are shown as mean ± standard error of the mean. *P <0.05, **P <0.01 versus PBS group; $^{\#}P$ <0.05, $^{\#\#}P$ <0.01 between PPP and PRP.

weeks after the injection, PRP-releasate induced restoration of disc height to the level approaching 90% of the non-punctured disc; this was sustained for the entire experimental period (4W, 6W, 8W: P <0.01 versus PBS group; 4W: P <0.05, 6W, 8W: P <0.01 versus PPP group) (Figure 2). While the PPP group also showed a significant recovery of disc height compared with the PBS group, it was no more than 80% of that of the non-punctured disc (4W, 6W, 8W: P <0.01 versus PBS group) (Figure 2). The injection of PBS did not induce restoration of disc height over the same time period (Figure 2).

Magnetic resonance imaging assessment

MRI analysis was performed at 8 weeks after the PBS, PPP, or PRP injections. Representative sagittal images of color-coded T2 maps showed that an area with high T2 value was identified in the NP injected with PRP-releasate (Figure 3). The normalized T2 values of the NPs (Figure 4a) were slightly higher than those for PPP (0.32 ± 0.03) and PRP (0.30 ± 0.02) samples compared with the values in the PBS samples (0.28 ± 0.02) but failed to reach statistical significance (P = 0.66). The normalized T2 values of the AFs (Figure 4b) showed similar trends, being somewhat higher for PRP (0.89 ± 0.08) and PPP (0.84 ± 0.06) compared with PBS control (0.70 ± 0.03). However, no statistically significant treatment effect was found (P = 0.49).

Histological evaluations

Safranin-O-stained histology in the PBS group (Figure 5c, d) showed severely degenerated discs in which most of the NP contents have been lost and collapsed, wavy fibrocartilage lamella and associated fibrochondrocyte-like cells of the AF. In the PPP and PRP groups, the increasing numbers of chondrocyte-like cells, which appear as large cells encircled with pericellular matrix densely stained with safranin-O, were found in either the inner AF or the NP (Figure 5f,h, respectively). However, there were no significant differences in the histological scores among the three groups. In all of the experimental groups, the invasion of blood vessels or inflammatory cells was not observed within the discs (Figure 5c,d, Figure 5e,f, and Figure 5g,h, respectively). Furthermore, no ossification of exclusively IVD tissues was found in any of the samples, although there was significant osteophyte formation at the edge of the vertebral body (Figure 5c,e,g).

Within the present study, one of the major cellular changes was the increasing number of chondrocyte-like cells in the inner AF or in the NP of PRP-releasate-injected discs, as previously reported [24]. In the anterior (inner) AF, the number of chondrocyte-like cells in the PRP group was significantly higher than those of the PBS and PPP groups (P <0.01) (Figure 5). The injection of the PRP-releasate significantly increased the number of chondrocyte-like cells in the NP compared with that of the PBS group (P <0.01), although no significant differences were found between the PRP and PPP groups (P = 0.06) (Figure 6). In the posterior (inner) AF, no significant differences were found among the three groups (Figure 6).

Discussion

This study examined the efficacy of the injection of PRP-releasate into degenerated discs in the well-established rabbit anular needle puncture model. The results of this study demonstrated that the intradiscal injection of PRP-releasate is effective for restoring disc height in this animal model. The histological analysis also revealed a reparative effect of PRP-releasate on the degenerated IVD.

Platelets have three major granule storage compartments: alpha granules, dense granules, and lysosomes. Alpha granules contain a large number of different secretory proteins, such as growth factors, coagulation proteins, adhesion molecules, cytokines, cell-activating agents, and angiogenic factors [18]. Platelets must be activated to release the contents of alpha granules to the external milieu where they exert potent biological effects. In many *in vitro* or *in vivo* studies (or both), activation of PRP is accomplished by adding bovine or human thrombin with calcium chloride [8,21,22,25-28]. However, it would be more feasible for clinical use if the concern about immunogenic reactions or disease transmission in using xenogeneic or allogeneic blood products were eliminated. In addition, the use of thrombin was of concern to us because thrombin has been shown to degrade cartilage tissues [29] and to cleave the same site as plasmin [30,31]. Therefore, in this study, we used a mixture of autologous serum and calcium chloride for activation of PRP.

The administration of PRP-releasate into degenerated IVDs greatly restored the decrease in disc height following anular needle puncture in this *in vivo* rabbit model. In a previous study using the same animal model, the injection of OP-1 [11] or growth differentiation factor-5 (GDF-5) [24] induced restoration of disc height to a level approaching 90% of that of a normal non-punctured disc. The results of our study suggest that the administration of PRP-releasate had an effect on the structural restoration of disc height similar to those of OP-1 or GDF-5 or both.

The major advantage of using PRP over purified growth factors is that PRP can be isolated from an autologous source, thus eliminating concerns about the potential for cancer [32] or autoantibodies. In addition, the preparation of PRP can be performed in a regular hospital setting with a minimum requirement for equipment and less vigorous regulatory oversight. However,

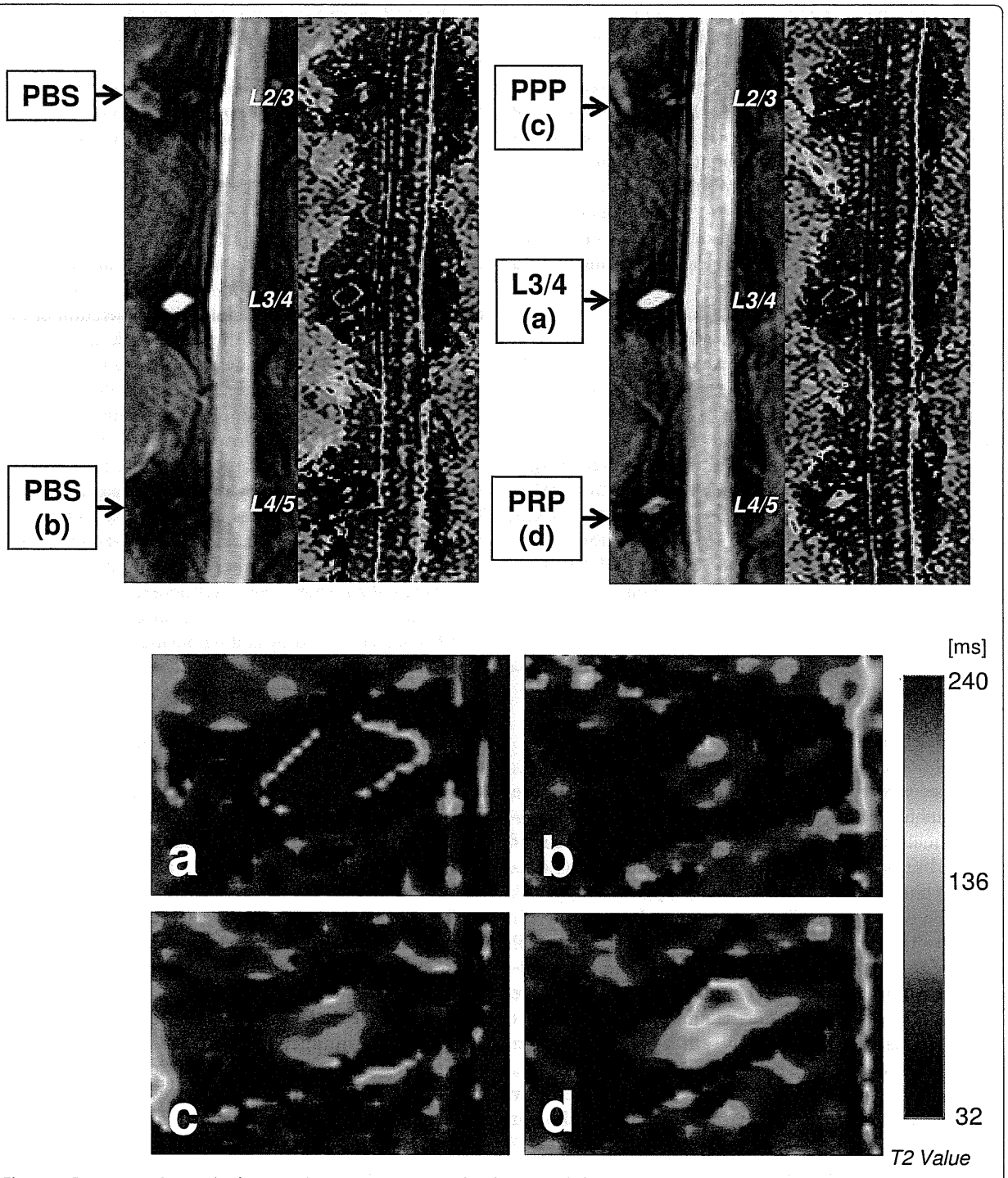

Figure 3 Representative sagittal magnetic resonance T2-weighted images (left panels) and T2 maps (right panels) of rabbit lumbar spines. The lower four images are magnifications (4×) of those discs in the upper two T2 maps: **(a)** non-punctured control (L3/4), **(b)** phosphate-buffered saline (PBS) (control) group, **(c)** platelet-poor plasma (PPP)-releasate group, and **(d)** platelet-rich plasma (PRP)-releasate group. The T2 values in the nucleus pulposus (NP) are significantly lower in all punctured discs (b-d) compared with non-punctured discs (a). However, areas with high T2 values area are identified in the center of the NPs injected with (c) PPP- and (d) PRP-releasates.

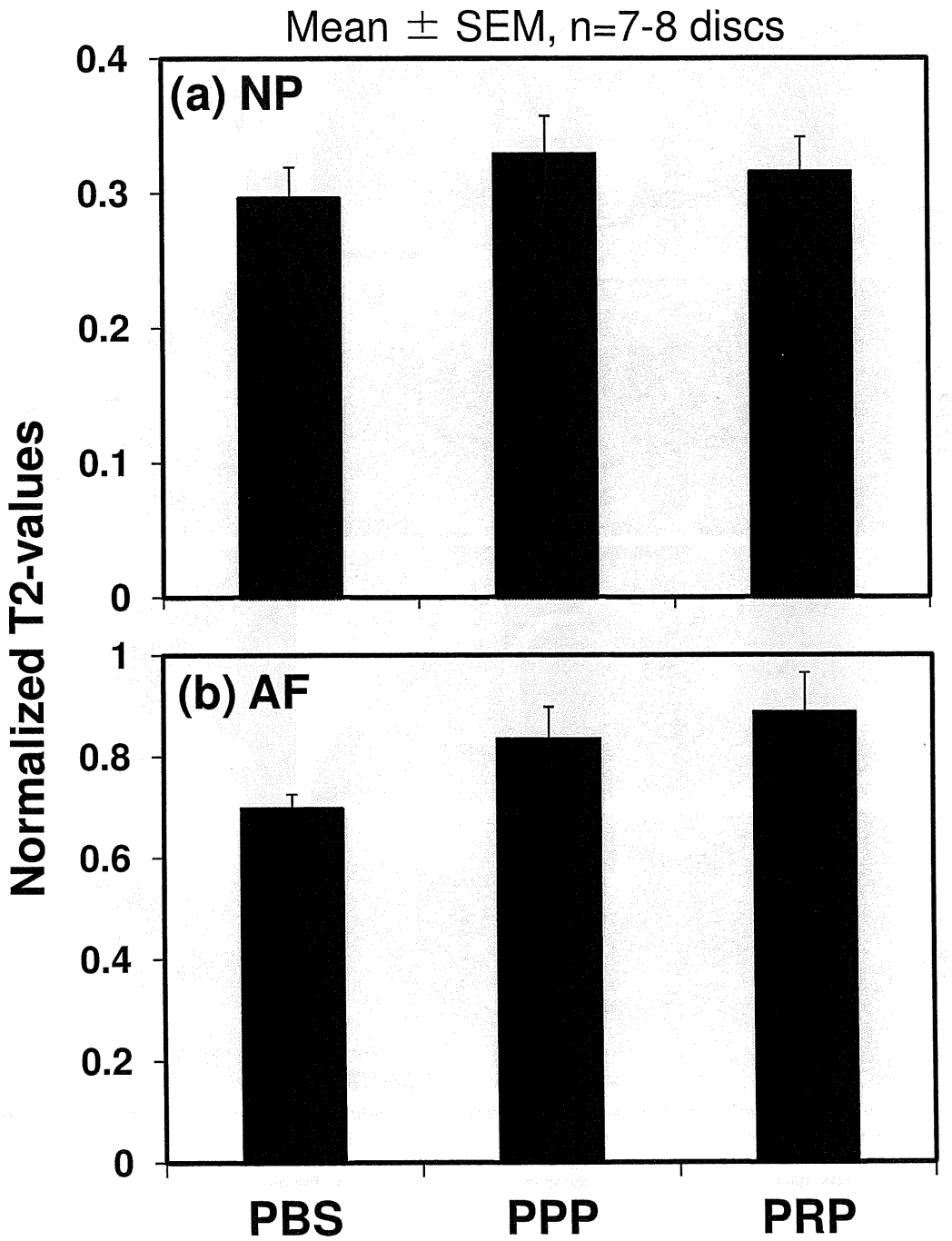

Figure 4 Magnetic resonance imaging results of normalized T2 values. Magnetic resonance imaging (MRI) analysis was performed at 8 weeks after the phosphate-buffered saline (PBS) (control), platelet-poor plasma (PPP)-releasate, and platelet-rich plasma (PRP)-releasate injections. The normalized T2 value of the PBS group was the lowest on average, but no statistical significance was found. Values are shown as mean ± standard error of the mean (SEM): PBS; n = 7 discs, PPP; n = 7 discs, PRP; n = 8 discs.

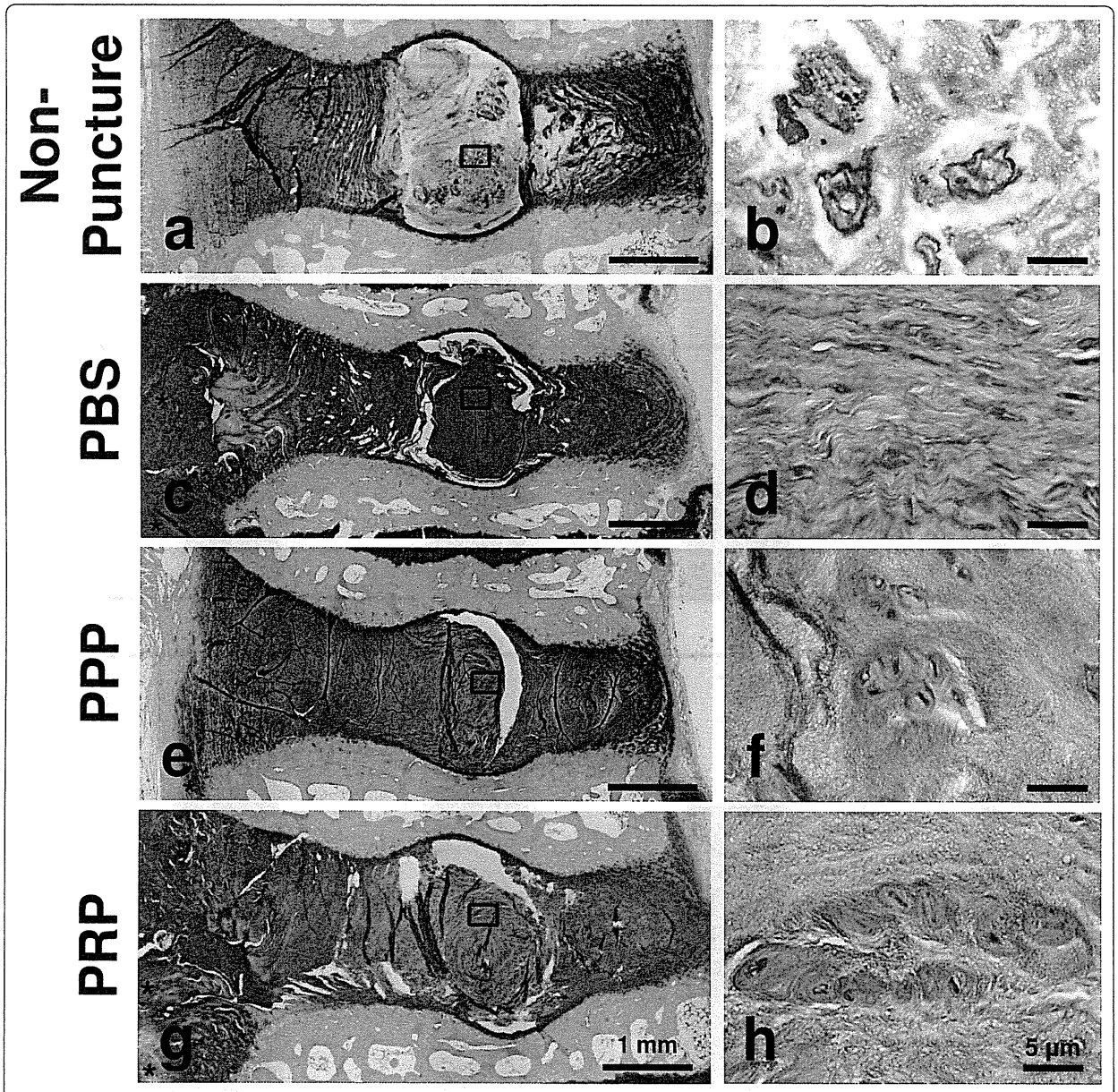

Figure 5 Typical histological changes after injections of phosphate-buffered saline (PBS) (c,d), platelet-poor plasma (PPP)-releasate (e, f), or platelet-rich plasma (PRP)-releasate (g,h). On safranin-O-stained sections, a moderate-to-severe degeneration was observed in the PBS (c,d) and PPP (e,f) groups. In the PRP group, the increasing number of chondrocyte-like cells which appeared as large cells encircled with pericellular matrix densely stained with safranin-O were found in the nucleus pulposus (h). The histology of the non-punctured control (L3/4) is shown in (a,b). (b,d,f,h) are magnification images of the area indicated by a square (a,c,e,g), respectively. Scale bars: 1 mm (a,c,e,g) and 5 μm (b,d, f,h). Asterisk indicates osteophyte formation.

the inter-individual variability in the concentration of growth factors found in PRP, compared with the well-controlled recombinant growth factors currently in clinical trials (OP-1 and GDF-5), may result in inconsistent effects.

MRI has recently been used not only for morphological evaluation but also for characterization of the structural organization and matrix content of the IVD. The T2 mapping technique has shown its potential to quantitatively evaluate changes in the molecular composition and structural organization of the IVD [33-36]. In our study, the T2 mapping technique was used to detect and quantify changes in the matrix structure and integrity of degenerated rabbit IVDs injected with PBS and